

Asymmetrical Distribution of Intrinsic Fluorescence Lifetimes in Proteins

Giampiero Mei,¹ Almerinda Di Venere,¹ Fabio De Matteis,² Alessandro Lenzi,³ and Nicola Rosato^{1,4,5}

Received April 16, 2001; revised July 19, 2001; accepted July 26, 2001

Dynamic fluorescence measurements of proteins in solution are often interpreted in terms of continuous distributions of lifetimes, which reflect the intrinsic structural heterogeneity of these systems. In several cases a single Gaussian or Lorentzian symmetric distribution has been used to fit the data. In this paper we describe a new nonsymmetric Lorentzian function which contains three free parameters (the center, the left, and the right widths) like the double-discrete exponential model (the two lifetimes and one preexponential factor). Simulated data in the frequency domain have been used to compare the fits obtained with these different approaches, introducing a new parameter, ρ , which quantitatively measures the asymmetry of the distribution or the ratio of the two preexponential factors, in the continuous and discrete models, respectively. Real measurements of a mixture of independent fluorophores, as well as of protein fluorescence decays, have also been performed and analyzed in terms of the new asymmetric function. The data have also been fitted with traditional discrete methods (such as the two- and the three-exponential decay) and with another asymmetric function, namely, the skewed Gaussian distribution.

KEY WORDS: Protein fluorescence decay; frequency domain fluorometry; distribution of lifetimes.

INTRODUCTION

Phase-shift and demodulation techniques are powerful methods for the investigation of protein conformational dynamics, through the emission fluorescence of intrinsic probes, such as tyrosine and tryptophan [1]. The

improvements in instrumentation and the development of powerful software for data analysis have clearly demonstrated that several proteins containing a single emitting fluorophore behave like heterogeneous systems, displaying an emission decay, $I(t)$, which cannot be satisfactorily fitted with a single-exponential function. Thus, a discrete two-/three-component decay function or, alternatively, a continuous distribution of lifetimes is often required to describe the fluorescence decay [2]. In the latter case two strategies have been developed to analyze the data. In the first algorithm, a set of fixed, equally spaced lifetimes is selected and then the preexponential factors of a multiexponential decay are varied, minimizing the chi-square (exponential series method) or the Shannon–Jaynes entropy function (maximum entropy method). In both cases no assumption is made on the shape of the lifetime distribution, which is instead given by the final profile of the best-fitting preexponential fac-

¹ Dipartimento di Medicina Sperimentale e Scienze Biochimiche and INFN Università di Roma “Tor Vergata,” Rome, Italy.

² Dipartimento di Fisica and INFN Università di Roma “Tor Vergata,” Rome, Italy.

³ Istituto di Chimica Quantistica ed Energetica Molecolare (ICQEM), CNR, Pisa, Italy.

⁴ AFaR-CRCCS Divisione di Neurologia, Ospedale San Giovanni Calibita, Fatebenefratelli, Rome, Italy.

⁵ To whom correspondence should be addressed at Department of Experimental Medicine and Biochemical Sciences, University of Rome “Tor Vergata,” Via di Tor Vergata 135, Rome 00133, Italy. Fax: +39 0672596468. E-mail: nicola.rosato@uniroma2.it

tors [3,4]. The second possibility is to start the analysis with a distribution whose analytical function is known a priori. The minimization algorithm is then used to search for those parameters (center and width of the distribution) which give the lowest chi-square value. Both Lorentzian and Gaussian-shaped distributions of lifetimes have been used to describe the fluorescence decay of proteins [5–7]. However, besides the predetermined form, other two limitations occur when using such functions. In fact, while a discrimination between a distributed and a single-exponential decay can be easily achieved, it is often difficult to make a clear distinction between a fit obtained with a Lorentzian- or Gaussian-shaped set of lifetimes and a double-exponential function. This comparison is also complicated by the presence of an intrinsic “statistical inconvenience”: the number of free parameters allowed to vary in the distribution fit is $k = 2$, while $k = 3$ in the case of a double-exponential model (two lifetimes and the ratio of the two preexponential factors). Moreover, both Lorentzian and Gaussian functions do not take into account an eventual “asymmetry” in the lifetime set which might characterize the emission decay. All these problems may be overcome by introducing asymmetric-shaped distributions. Indeed the usefulness of asymmetric functions in the interpretation of fluorescence data has already been proved. For example, in 1991 Wiczak and co-workers [8] successfully employed a skewed Gaussian function to represent the donor–acceptor distance distributions obtained in fluorescence energy transfer measurements.

Since in the past years most of the protein fluorescence decays obtained by phase fluorometry have been interpreted in terms of Lorentzian lifetime distributions [9–19], we decided to simulate experimental data with an asymmetrical Lorentzian function. In this paper we report a comparison between this new asymmetric distribution and the double-exponential decay, which share the same number of free parameters ($k = 3$). The quality of both fitting functions was investigated through the better residuals pattern and the minimum chi-square value reached in each case. A detailed analysis of the reduced chi-square surfaces is reported for each fit, obtaining the confidence interval of the parameters used. The limits of the symmetric Lorentzian compared to both the asymmetric distributed function and the double-exponential model are also discussed. The new nonsymmetric function is used to fit the fluorescence decay of selected proteins, namely, bacterial superoxide dismutase (PSOD), phosphofructokinase (PFK), and bovine superoxide dismutase (BSOD), studying the emission of both tryptophans (in the first two cases) and tyrosines (in the case of BSOD).

Finally, both simulated and experimental data are analyzed in terms of a skewed Gaussian distribution of lifetimes, and the results compared to those obtained with the nonsymmetric Lorentzian function.

MATERIALS AND METHODS

Theory

The fluorescence decay associated with a δ -pulse excitation has commonly been described by a sum of discrete exponentials,

$$I(t) = \sum_{i=1}^n \alpha_i e^{-t/\tau_i} \quad (1)$$

or, alternatively, by a continuous distribution of fluorescence lifetimes,

$$I(t) = \int_0^{\infty} \alpha(\tau) e^{-t/\tau} d\tau \quad (2)$$

where α_i and $\alpha(\tau)$ represent the discrete and continuously distributed preexponential factors, respectively. In the past years, the latter model has been used [7,20] to characterize the distribution of lifetimes with a Lorentzian-shaped preexponential function:

$$\alpha(\tau) = \frac{(w/2)^2}{(\tau - c)^2 + (w/2)^2} \quad (3)$$

where c and w correspond to the center and full width at half-maximum (FWHM) of the distribution. From Eq. (3), it follows that the lifetimes $\{\tau\}$ are symmetrically disposed around a central value $\tau = c$. To fit the data with an asymmetric function, we modified Eq. (3) so that

$$\alpha_L(\tau) = \frac{(w_L/2)^2}{(\tau - c)^2 + (w_L/2)^2}, \quad \tau \leq c; \quad (4)$$

$$\alpha_R(\tau) = \frac{(w_R/2)^2}{(\tau - c)^2 + (w_R/2)^2}, \quad \tau \geq c$$

where $w_L/2$ and $w_R/2$ are the left and right side of the FWHM, respectively. We call this function JANUS, since it is a distribution with two distinct sides. We also defined a new parameter, $\rho_J = w_R/w_L$, which measures the “degree of asymmetry” of a JANUS distribution. When $\rho_J = 1$ the JANUS model is coincident with a Lorentzian symmetric function.

The fractional fluorescence contribution of each emitting species with lifetime τ , $F(\tau)$, has often been reported instead of $\alpha(\tau)$; for this reason we wrote a pro-

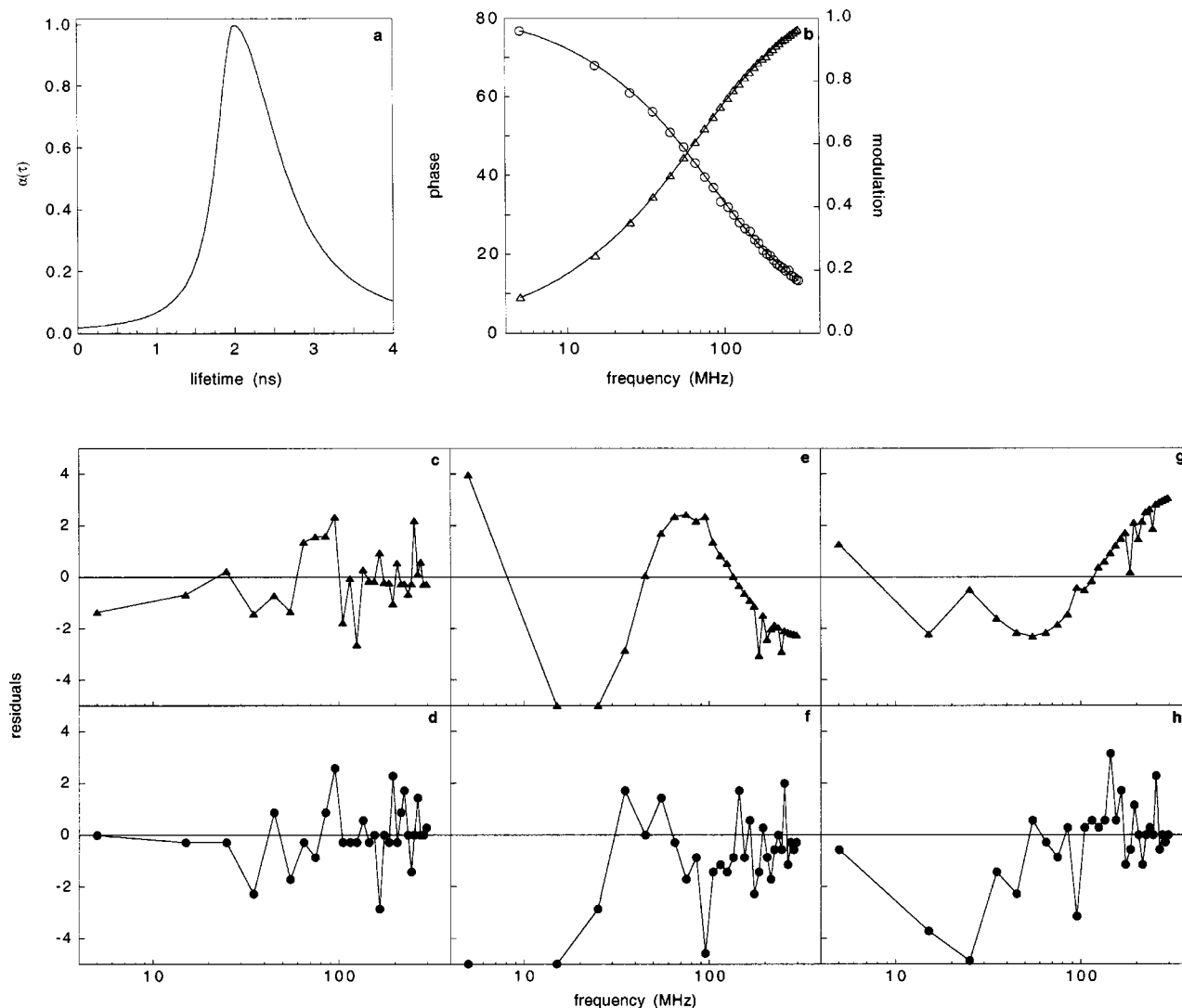


Fig. 1. (a) Shape of the simulated JANUS function using $c = 2$ ns, $w_L/2 = 0.27$ ns, and $w_R/2 = 0.68$ ns. (b) Simulated phase-shift and demodulation data (obtained with the distribution in a) as a function of the modulation frequency. The solid line represents the best fit (see first line in Table I). (c–h) Weighted residuals of phase (triangles) and modulation (circles) data fitted with a JANUS (c, d), double-exponential (e, f), or symmetric Lorentzian (g, h) model.

gram (in Pascal language) with a routine which can also use, in expression (2), both $F(\tau)/\tau$ and the preexponential factors, $\alpha(\tau)$. This option has been included in the analysis of the data with the JANUS distribution, Eq. (4).

In frequency-domain techniques the measured phase-shift and demodulation values at each frequency, ϕ_ω and m_ω are correlated with the sine and cosine transforms of the decay function through the equations

$$\phi_\omega = \arctan \frac{N_\omega}{D_\omega}$$

$$m_\omega = \sqrt{N_\omega^2 + D_\omega^2}$$

where

$$N_\omega = \int_0^\infty I(t) \sin \omega t \cdot dt / \int_0^\infty I(t) \cdot dt$$

$$D_\omega = \int_0^\infty I(t) \cos \omega t \cdot dt / \int_0^\infty I(t) \cdot dt$$

Table I. Fluorescence Dynamics Parameters Obtained Fitting the Simulated Data in Figs. 1b, 2b, and 3b^a

Simulated with	Fitted with													
	JANUS				Two exponentials				Lorentzian					
	χ^2	C (ns)	$w_L/2$ (ns)	$w_R/2$ (ns)	χ^2	τ_1 (ns)	τ_2 (ns)	α_1 (%)	χ^2	C (ns)	w (ns)			
JANUS	1.1	2.04	-0.27	-0.13	-0.03	6.6	2.17	-0.13	-0.56	-0.05	3.2	2.40	-0.14	-0.11
			+0.14	+0.09	+0.02			+0.20	+3.74	+0.06			+0.09	+0.09
			-0.27	-0.64	-0.04			-0.05	-0.08	-0.04			-0.17	-0.08
Two exponentials	5.0	1.82	1.38	0.24	0.9	0.79	2.18	0.54	18.3	1.25	0.51			
			+0.12	+2.10	+0.03			+0.02	+0.12	+0.06			+0.18	+0.10
			-0.15	-0.05	-0.03			-0.46	-0.81	-0.14			-0.03	-0.03
Lorentzian	1.3	1.96	0.65	0.70	15.0	1.70	6.42	0.78	1.3	1.99	1.41			
			+0.18	+0.14	+0.02			+0.26	+1.98	+0.22			+0.02	+0.05

^a χ^2 : reduced chi-square value. C , τ_1 , τ_2 : center of the distribution or discrete lifetime value. α_1 : preexponential factor of the first component ($\alpha_1 + \alpha_2 = 1$). w_L , w_R , w : width of the lifetime distribution.

To fit the data with different fluorescence decays, $I(t)$, the program minimizes the reduced chi-square function,

$$\chi^2 = \frac{1}{\nu} \left[\sum_{\omega} \left(\frac{(\phi_{\omega} - \phi_{\omega}^c)^2}{(\Delta\phi)^2} + \frac{(m_{\omega} - m_{\omega}^c)^2}{(\Delta m)^2} \right) \right]$$

by a nonlinear least-squares routine, based on the Marquardt–Levenberg algorithm, where ν is the number of degrees of freedom, ϕ^c and m^c are the calculated phase and modulation values, and $\Delta\phi$ and Δm represent the uncertainties in the measured data. The integrals N_{ω} and D_{ω} can be calculated by the program both numerically and by analytical formulas which can be obtained by exchanging the order of integration between t and τ . In the latter case the upper limit in the lifetime integral can also be fixed a priori, as in the numerical calculation, truncating the Lorentzian right tail to a maximum value (which can be, for example, the unquenched radiative lifetime of the excited state, τ_0). The simulated data were obtained by fixing the decay function, $I(t)$, and adding to the calculated phase and modulation values (ϕ_{ω} and m_{ω}) a Gaussian noise, using a Monte Carlo double-extraction algorithm. The set of frequencies (≥ 30) ranged from $\nu \approx 5$ to $\nu \approx 300$ MHz, since the mean lifetime was about 1.5–2.0 ns.

Samples

Aniline, 2-(1-naphthyl)-5-phenyloxazole (α -NPO), anthracene, 1,4-bis(5-phenyl-2-oxazolyl)benzene (POPOP), and *p*-terphenyl were purchased from Fluka and dissolved in ethanol. Purified PSOD was a generous gift from the laboratory of Dr. Alessandro Desideri. PFK was purchased from Sigma. All samples were thermostated at 20°C during

the measurements using an external bath circulator. The phase and modulation data of BSOD were obtained from Ferreira *et al.* [13].

Fluorescence Measurements

Dynamic fluorescence measurements were performed using the phase-shift and demodulation technique [21]. The excitation source ($\lambda_{\text{ex}} \approx 293$ nm) was a frequency-doubled rhodamine 6G–NdYag laser, while emission was collected through a WG 320 cutoff filter to avoid scattered light. A minimum of 22 frequencies was employed in each measurement.

Fits

The quality of the different fits was checked by the lower chi-square value, according to the F -test statistics [22]. The Smirnov–Kolmogorov test [23] was applied to the weighted residuals to check for their Gaussian distribution around zero.

The fits obtained using the skewed Gaussian function were performed using the software produced by M. L. Johnson and available on-line at the Center for Fluorescence Spectroscopy site (cfs.umbi.umd.edu).

RESULTS AND DISCUSSION

Analysis of Simulated Fluorescence Decays

A typical profile of a JANUS distribution of lifetimes, with $p_j > 1$, is reported in Fig. 1a. The correspond-

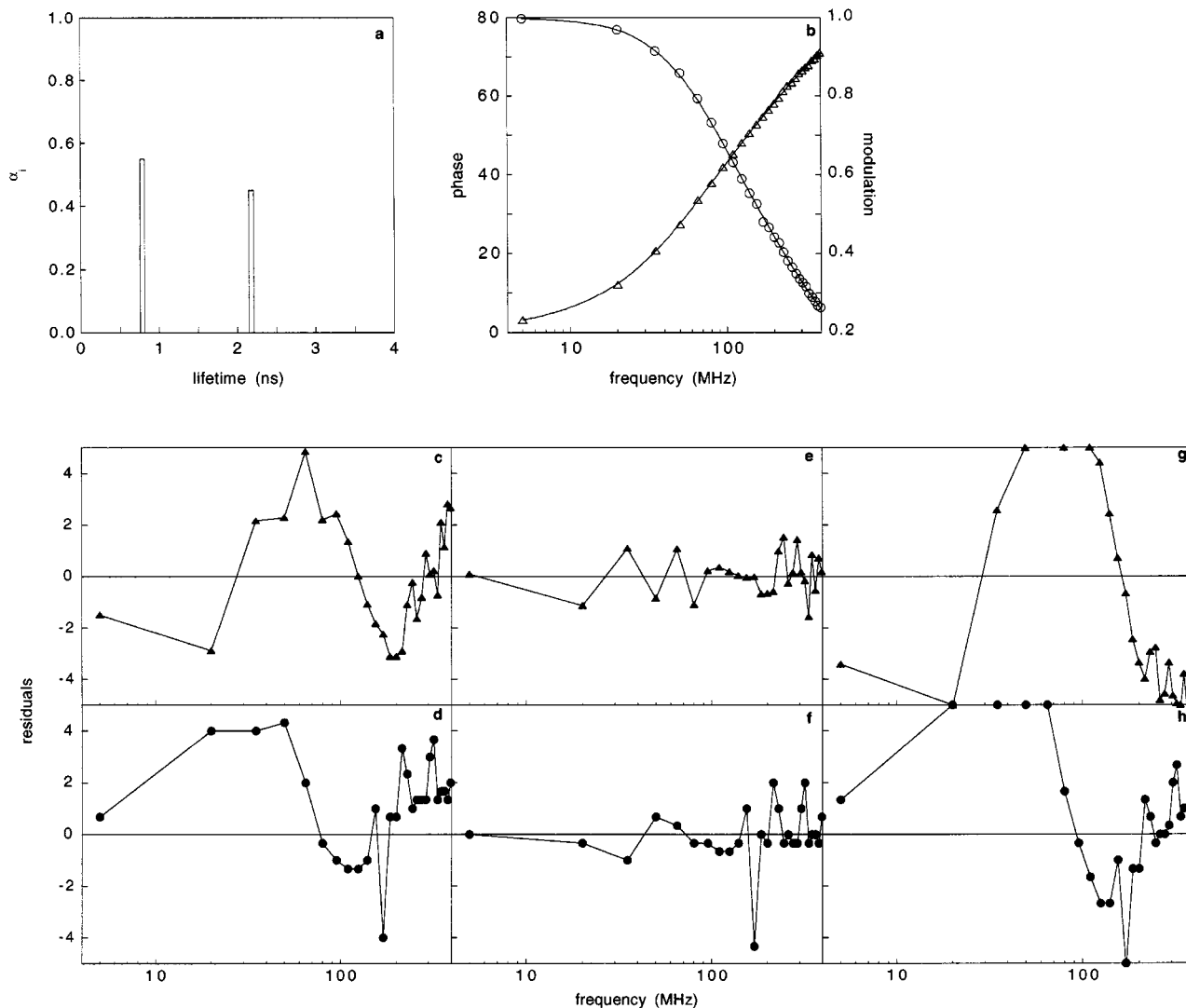


Fig. 2. (a) Lifetimes ($\tau_1 = 0.8$ ns, $\tau_2 = 2.2$ ns) and preexponential factors ($\alpha_1 = 0.55$, $\alpha_2 = 0.45$) used to simulate a double-exponential fluorescence decay. (b) Simulated phase-shift and demodulation data (obtained with the values in a) as a function of the modulation frequency. The solid line represents the best fit (see second line in Table I). (c–h) Weighted residuals of phase (triangles) and modulation (circles) data fitted with a JANUS (c, d), double-exponential (e, f), or symmetric Lorentzian (g, h) model.

ing phase and demodulation data (Fig. 1b) were simulated from the decay function, $I(t)$ (see Materials and Methods), and then fitted with both nonsymmetric and symmetric Lorentzians or with a two-discrete exponential decay. The results of this analysis are reported in the first line in Table I, while the weighted residuals of each fit are shown in Figs. 1c–h. According to the F -test statistics (with a 0.05 confidence limit), the chi-square values obtained with the JANUS function are significantly lower than those of other fits. Also, the Smirnov–Kolmogorov test of the weighted residuals demonstrates that only those

reported in Figs. 1c and d are distributed around zero according to a Gaussian statistics (with $\mu = 0$ and $\sigma = 1$).

We also performed simulations for a double-exponential decay (Fig. 2a) and for a Lorentzian-distributed ensemble of lifetimes (Fig. 3a). In the first case it is not possible to obtain a lower chi-square value or a better residuals pattern than that of a discrete model, using distributions (see the second line in Table I and Fig. 2). On the other hand, as demonstrated in Table I, line 3, and Fig. 3, two lifetimes are not sufficient to fit the data obtained from a Lorentzian distribution, while the JANUS

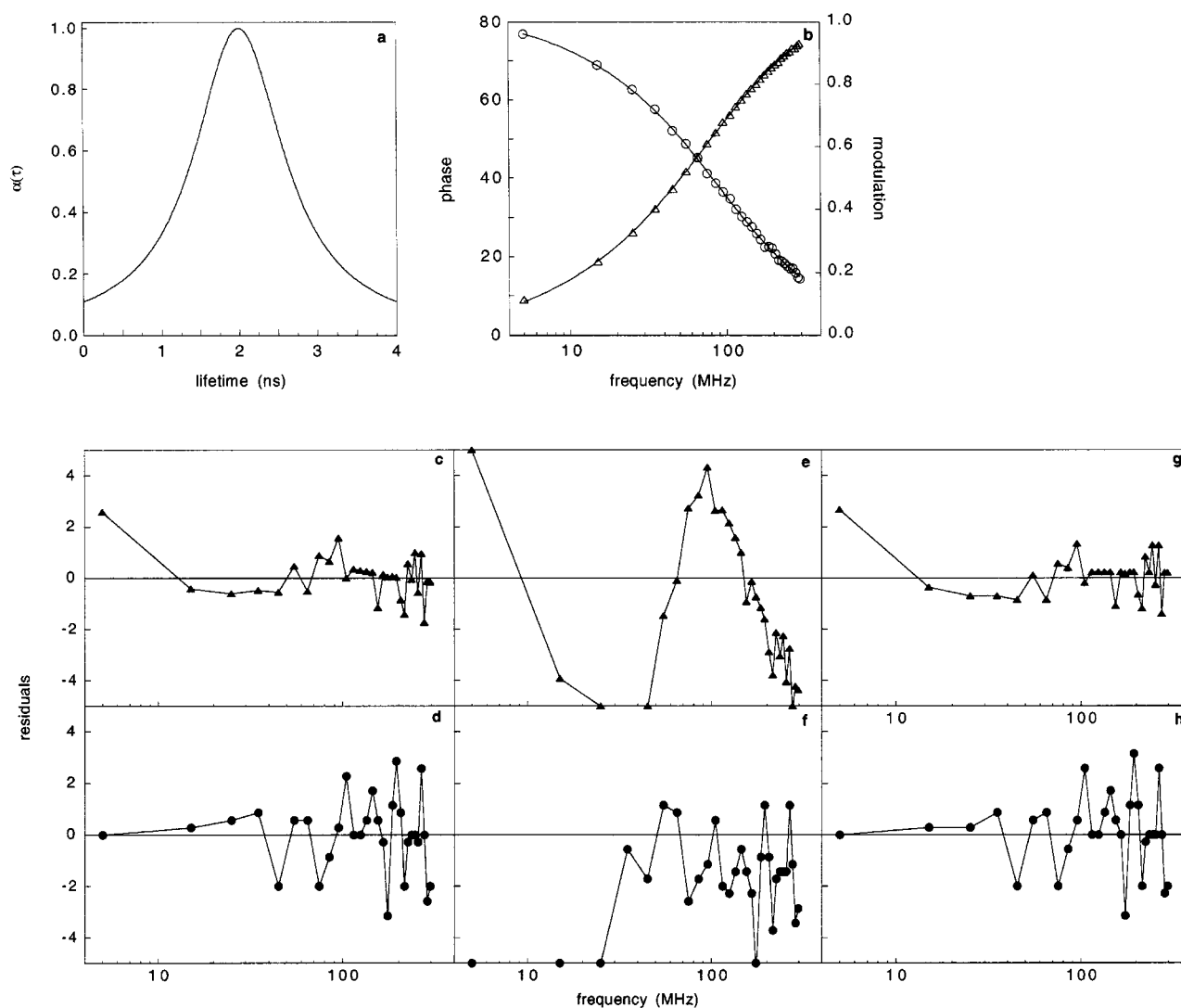


Fig. 3. (a) Shape of the simulated symmetric Lorentzian function using $c = 2$ ns and $w = 1.4$ ns. (b) Simulated phase-shift and demodulation data (obtained with the distribution in a) as a function of the modulation frequency. The solid line represents the best fit (see third line in Table I). (c–h) Weighted residuals of phase (triangles) and modulation (circles) data fitted with a JANUS (c, d), double-exponential (e, f), or symmetric Lorentzian (g, h) model.

model gives a result which cannot be distinguished from the symmetrical distribution: the sum of the right and left half-widths ($0.65 + 0.70$ ns) is in fact close to the full width used for the simulation (1.40 ns).

A more accurate comparison between the results of the double-exponential and the asymmetric fitting function was carried out evaluating the confidence interval of each parameter used to fit the data. This analysis was performed examining the reduced chi-square surfaces obtained fixing one parameter per time and adjusting the others to reach a minimum chi-square value. The results of this procedure are shown in Figs. 4 and 5. The errors associated with

each parameter, according to a 90% confidence interval (see Figs. 4 and 5), are reported in Table I. As expected, the parameters are determined with a good accuracy only when the fit is performed with the corresponding function used in the simulation. This result suggests that it is possible to discriminate (at least in this case) among asymmetric, symmetric, or discrete decay models.

In the three examples shown, the parameters of the simulated decays were chosen arbitrarily, although in the range of a few nanoseconds, to simulate tryptophan or tyrosine dynamic fluorescence in proteins. Of course, the choice of the two discrete lifetimes as well as the widths

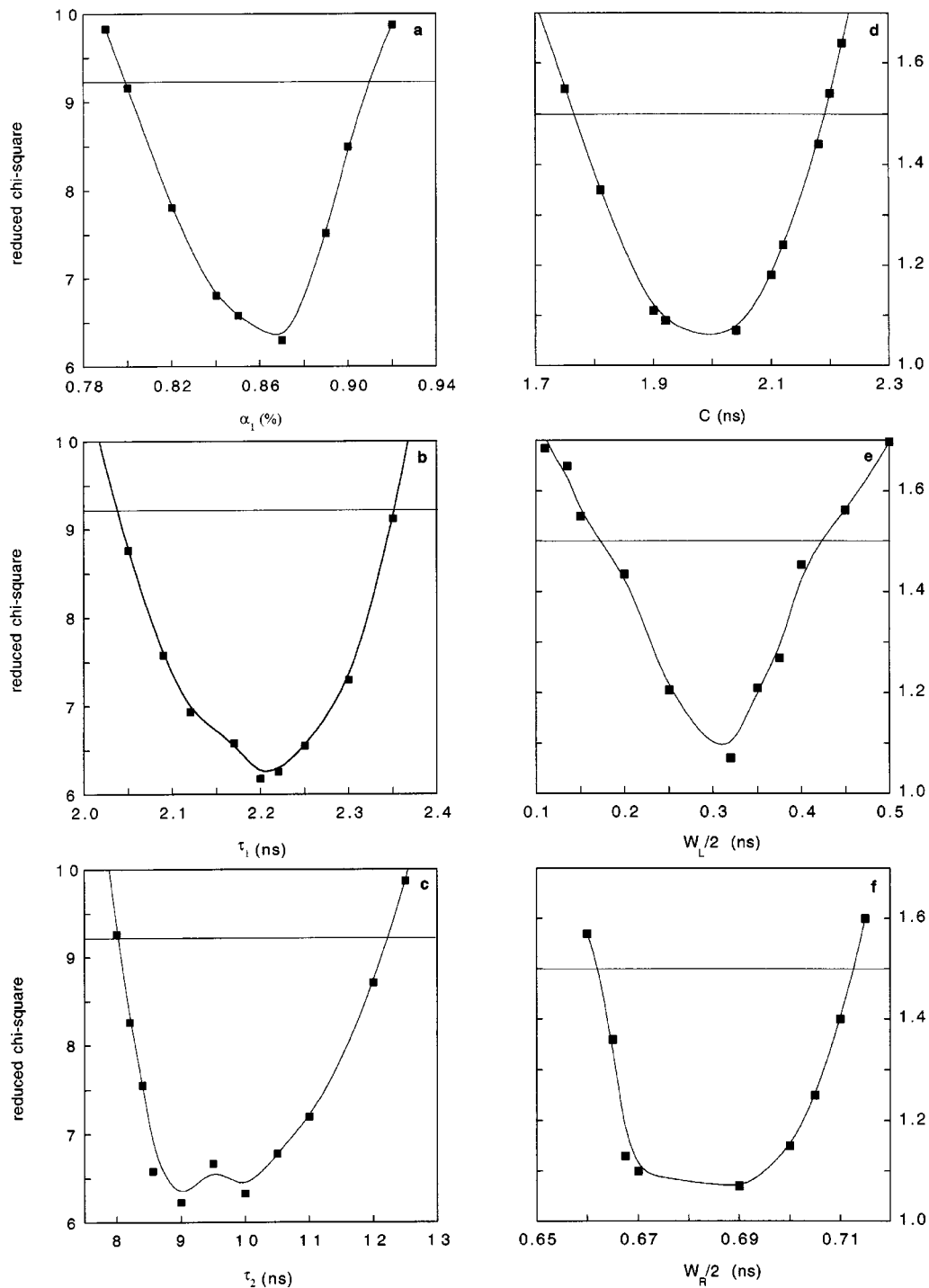


Fig. 4. Chi-square surfaces obtained fitting the phase and modulation data reported in Fig. 1b, with a double-exponential model (a–c) or a JANUS distribution of lifetimes (d–f). The uncertainties of the parameters reported in Table I were evaluated according to the 90% confidence intervals indicated by the horizontal lines.

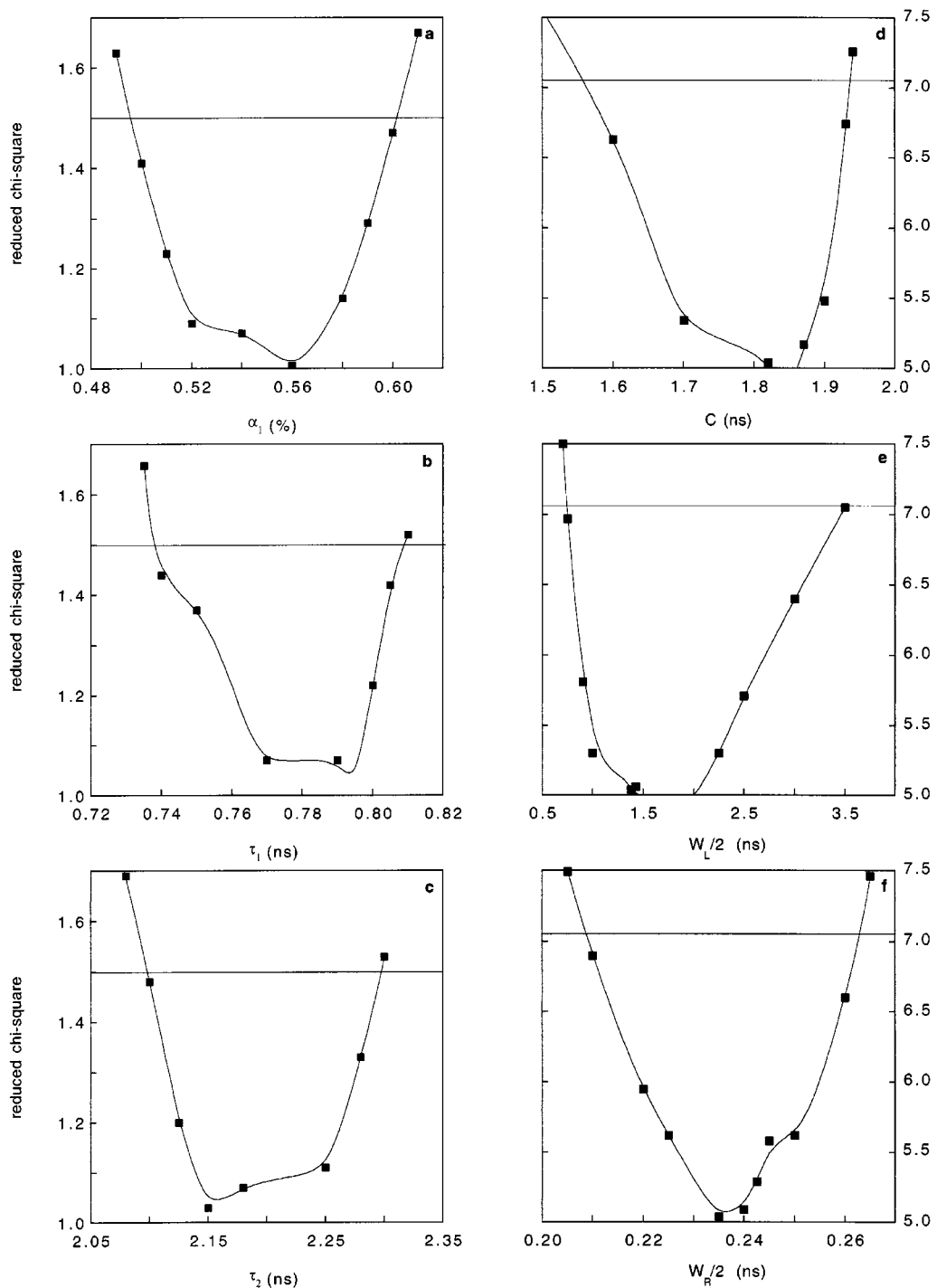


Fig. 5. Chi-square surfaces obtained fitting the phase and modulation data reported in Fig. 2b, with a double-exponential model (a–c) or a JANUS distribution of lifetimes (d–f). The uncertainties of the parameters reported in Table I were evaluated according to the 90% confidence intervals indicated by the horizontal lines.

of the distributions might be critical for the better quality of one particular fit compared to the others. For example, it might be expected that a shorter interval between the two lifetimes in Fig. 2a could reduce the chi-square value of the distributions fits, giving much narrower widths than those reported in Table I (second line). In the same way, two discrete exponentials should fit the data much better simulated with narrower Lorentzian functions than those reported in Figs. 1a and 3a. Furthermore, the quality of the different fitting models may be also influenced by another important property of the lifetimes ensemble, $\{\tau\}$, chosen to simulate the dynamic fluorescence data: the eventual asymmetry in the preexponential factors. At this regard we introduced both the asymmetry of two discrete lifetimes and that of a JANUS distribution (see Materials and Methods). Then we have simulated several data sets, varying the ratio of the preexponential factors, $\rho_D = \alpha_2/\alpha_1$, or the ratio of the two widths, $\rho_J = w_R/w_L$, in the discrete or in the JANUS model, respectively, keeping constant the lifetime values (τ_1 and τ_2), the center (C), and the full width $(w_L + w_R)/2$ of the distribution. The data were fitted with the three decay models and the respective chi-square values are reported in Fig. 6.

First, let us discuss the analysis of the simulations obtained with the two discrete lifetimes, varying, ρ_D , the asymmetry of the two preexponential factors (Fig. 6a). In this case the worst chi-square values were obtained when $\alpha_1 \approx \alpha_2$ (i.e., $\rho_D \approx 1$), fitting the data with both symmetric and asymmetric distributions of lifetimes. When one of the two preexponential factors was considerably larger than the other (i.e., $\rho_D \gg 1$ or $\rho_D \ll 1$), no difference with the discrete fit was observed (Fig. 6a). A reduced difference between the two lifetime values (Figs. 6b and c) produced a considerable improvement in the quality of the distributed fits.

Simulations obtained with the Janus function (Fig. 6d) could be satisfactorily fitted with a symmetric Lorentzian only when $\rho_J \approx 1$, i.e., when $w_L = w_R$. The double-exponential fit gave high chi-squares for almost all ρ_J values. However, when the simulations were repeated with narrower full widths of the JANUS function (Figs. 6e and f), the difference in the three fits was considerably reduced.

In conclusion, a clear discrimination between an asymmetric Lorentzian function and two discrete lifetimes was possible in two cases: when the simulation was performed with large distributions of lifetimes (Figs. 6d and e), or when the decay was simulated using two lifetimes far apart from each other (Figs. 6a and b), with similar preexponential factors ($\rho_D \approx 1$).

Similar results were also obtained by changing the center of the JANUS distribution and the average lifetime of the discrete model in the range 1–5 ns (data not shown).

Analysis of a Mixture of Fluorophores

To test the quality of the JANUS fitting function on experimental phase and demodulation data, we attempted to reproduce real asymmetrically distributed fluorescence decay using a mixture of noninteracting fluorophores. Five fluorescent molecules were selected with a single-exponential decay in the range of a few nanoseconds, obtaining the following results and reduced chi-square values when measured independently: *p*-therphenyl ($\tau = 1.03$ ns, $\chi^2 = 1.0$), POPOP ($\tau = 1.33$ ns, $\chi^2 = 1.1$), α -NPO ($\tau = 2.08$ ns, $\chi^2 = 1.1$), aniline ($\tau = 2.65$ ns, $\chi^2 = 1.5$), and anthracene ($\tau = 4.62$ ns, $\chi^2 = 1.1$). Then three mixtures of POPOP and anthracene were prepared (90:10, 85:15, and 75:25%) to obtain double-exponential decays with different preexponential factors (Table II). When the phase-shift and demodulation data for each mixture were analyzed in terms of distributed lifetime models, the best-fitting functions reported in Fig. 7 were obtained (see also Table II). Using the JANUS function, a low chi-square value was obtained only when a strong asymmetry in the two discrete lifetimes ($\rho_D \approx 0.075$; Fig. 7a) was present. In fact, as observed in the case of simulated data (Figs. 6a–c), the quality of the fit is worse when the two discrete lifetimes have more similar preexponential factors (Figs. 7b and c and Table II).

More complex fluorescence decays were obtained using mixtures of all five fluorophores. In Fig. 8 three distinct situations are shown corresponding to different relative concentrations of the five molecules (filled bars). The results of the data analysis reported in Table III clearly show the better quality of the JANUS function in fitting the measured phase and modulation data. Actually, both the discrete and the Lorentzian distribution display a trend in their calculated chi-square values as the asymmetry is increased from $\rho_J \approx 0.4$ to $\rho_J \approx 5.8$. On the other hand, the right width of the asymmetrical distribution correctly increases, as the longer-lifetime components (aniline and anthracene) become more important (Figs. 8b and c).

Analysis of Protein Decays

To test the quality of the JANUS model as a new fitting function for tryptophan and tyrosine fluorescence decay, we measured the fluorescence dynamics of three single fluorophore-containing proteins: bovine and bacterial superoxide dismutase (BSOD, PSOD) and phospho-

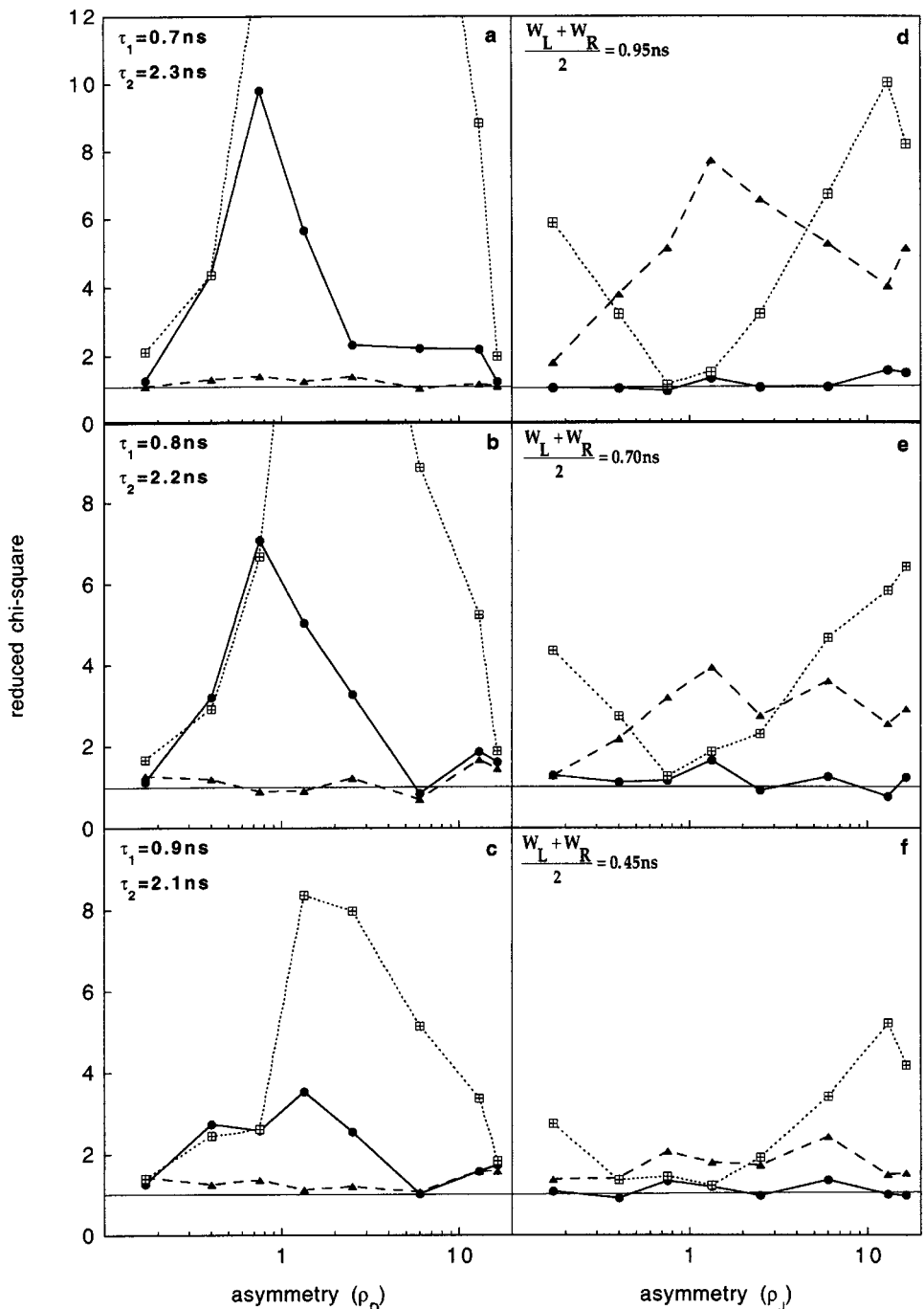


Fig. 6. Reduced chi-square values obtained fitting simulated data with a JANUS function (circles), two discrete exponentials (triangles), and a symmetric Lorentzian distribution (squares). The results reported in a–c correspond to the best fits of phase and modulation data simulated with double-exponential decay functions. Those reported in d–f are the best chi-squares obtained fitting the data simulated with different JANUS functions (centered at $C = 2 \text{ ns}$).

fructokinase (PFK). The best-fit parameters are reported in Table IV.

BSOD is a dimer of two identical subunits, each

containing a single tyrosine residue whose emission decay has been studied by Ferreira *et al.* [13] and fitted by both discrete and continuous lifetime models. Despite the

Table II. Fluorescence Decay Parameters for Three Mixtures of POPOP/Anthracene^a

Sample	JANUS				Two exponentials				Lorentzian		
	χ^2	C (ns)	$w_L/2$ (ns)	$w_R/2$ (ns)	χ^2	τ_1 (ns)	τ_2 (ns)	α_1 (%)	χ^2	C (ns)	w (ns)
Fig. 7a ($\rho_D = 0.08$)		-0.08	-0.03	-0.04	-0.10	-0.47	-0.06		-0.13	-0.11	
	1.7	1.14	0.04	0.22	1.0	1.34	4.81	0.93	2.9	1.36	0.49
		+0.10	+0.02	+0.05	+0.08	+0.14	+0.06		+0.10	+0.10	
Fig. 7b ($\rho_D = 0.16$)		-0.18	-0.02	-0.05	-0.05	-0.38	-0.05		-0.15	-0.09	
	3.5	1.12	0.03	0.32	1.0	1.34	4.71	0.86	4.8	1.43	0.77
		+0.19	+0.02	+0.07	+0.09	+0.22	+0.06		+0.16	+0.21	
Fig. 7c ($\rho_D = 0.32$)		-0.25	-0.05	-0.11	-0.06	-0.24	-0.04		-0.14	-0.13	
	19	1.25	0.05	0.47	1.2	1.35	4.96	0.76	15	1.69	1.11
		+0.38	+0.03	+0.12	+0.06	+0.42	+0.08		+0.12	+0.25	

^a χ^2 : reduced chi-square value. C , τ_1 , τ_2 : center of the distribution or discrete lifetime value. α_1 : preexponential factor of the first component ($\alpha_1 + \alpha_2 = 1$). w_L , w_R , w : width of the lifetime distribution.

lower chi-square value found using a double-exponential function, the authors preferred a Lorentzian-distributed decay, on the basis of an F -statistical analysis [13]. In Table IV we report both the parameters obtained by traditional methods and the results achieved with the JANUS distribution. With the asymmetric function an improvement in the chi-square value was obtained, despite its being at the limit of the F statistics (5% confidence), with respect to the Lorentzian function. A better discrimination between the JANUS and the Lorentzian comes from the analysis of weighted residuals: in fact the Smirnov–Kolmogorov test demonstrates that only in the first case are residuals randomly distributed around zero. Interestingly, with the JANUS a relevant asymmetry ($\rho_j \approx 1.93$) in the shape of the lifetime distribution was obtained (Table IV).

Like BSOD, the bacterial PSOD from *Photobacterium leiognathi* is also a homodimer but contains a buried tryptophilic residue per subunit [18]. The dynamic fluorescence of the apoprotein has recently been studied by phase-shift and demodulation techniques and the emission decay has been interpreted in terms of a Lorentzian distribution of lifetimes, centered around 1.3 ns [18] (Table IV). In this case no improvement in the quality of the fit was obtained using the JANUS function (Table IV), which in fact is characterized by an asymmetry value close to 1 and by a full width [$(w_L + w_R)/2 = 1.04$ ns] identical to that obtained with the symmetrical Lorentzian. This result, which could be expected on the basis of the low chi-square value already obtained with two free parameters in the fit (center and width), is important because it demonstrates that the JANUS and the Lorentzian give the same results when $\rho_j = 1$.

The fluorescence dynamics of PFK from *Bacillus stearothermophilus* has been investigated by Barkley and co-workers and the emission decay of the single tryptophan residue was fitted using a double-exponential function [24]. In this case the analysis of chi-square values and residuals reveals that it is not possible to fit the data using both symmetric and nonsymmetric Lorentzian functions (Table IV).

The three cases just discussed were considered to compare the results of two fitting functions which contain only three free parameters, namely, the double-exponential decay and the JANUS model. However, it is well known that proteins in solution exhibit an ensemble of interconverting conformational substates, and very often, more than two discrete lifetimes are required to fit protein fluorescence decays adequately [25]. In this regard, we also attempted to analyze the data using a three-exponential decay. The best fluorescence lifetime sets obtained for BSOD, PSOD, and PFK are reported in Fig. 9 together with the weighted residuals and the results obtained with the JANUS analysis (Table IV).

In all cases the analysis of residuals demonstrates that the asymmetric Lorentzian fit can hardly be distinguished from the discrete analysis. However, it is worth mentioning that in the new function there are only three free parameters, while five variables are used in the three-exponential decay.

The Skewed Gaussian

The skewed Gaussian is another nonsymmetrical function, which can also be used to fit heterogeneous spectroscopical processes in proteins [8]. Like the

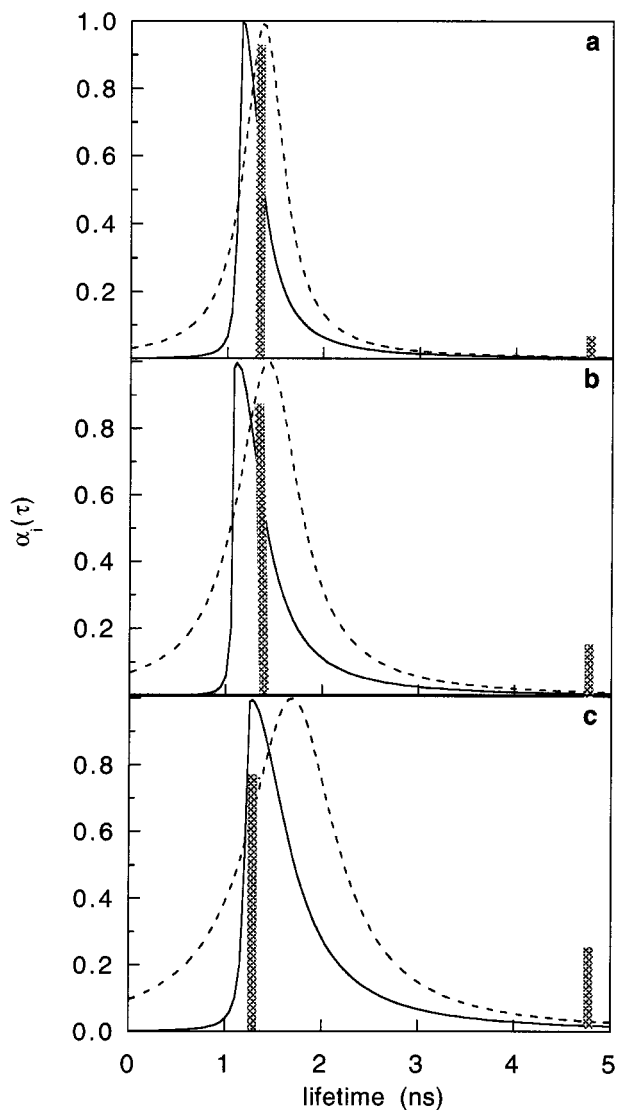


Fig. 7. Profile of the JANUS (solid line) and the symmetric Lorentzian (dashed line) distributions used to fit a fluorescence decay obtained by mixing two monoexponential fluorophores (filled bars).

JANUS function, it contains only three free parameters, namely, the center and width of the distribution (C , W) and the skewness (S), a parameter which indicates the asymmetry of the Gaussian distribution ($S = 0$ for a symmetrical function). In Table V the results of the fits obtained with the skewed Gaussian for both simulated and experimental data are reported. The high chi-square values reported in the first and third lines in Table V demonstrate that (in these cases) the skewed Gaussian could not be used to fit the data simulated with Lorentzian-shaped functions. A similar result was obtained using symmetric and nonsymmetric Lorentzi-

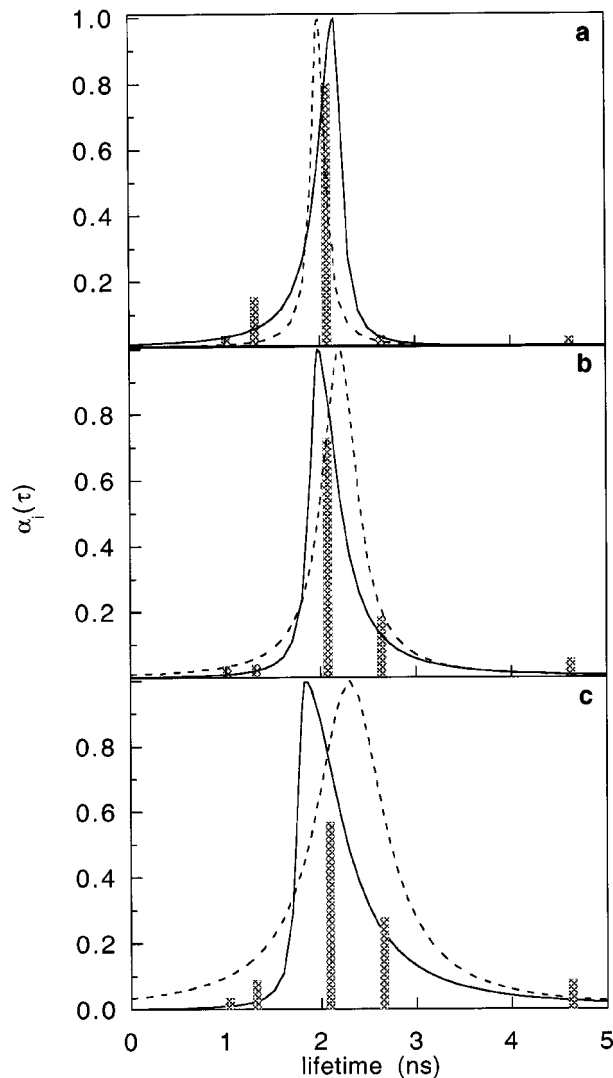


Fig. 8. Profile of the JANUS (solid line) and the symmetric Lorentzian (dashed line) distributions used to fit a fluorescence decay obtained by mixing five monoexponential fluorophores (filled bars).

ans to fit the data simulated with a skewed Gaussian (data not shown). In the case of a mixture of fluorophores, the JANUS fit and the skewed Gaussian give similar results, as long as the asymmetry is low (lines 4 and 5 in Table V). As expected, when the asymmetry in the lifetime fractions increases (see Fig. 8) a corresponding increase in the skewness value can be observed (from line 4 to line 6 in Table V). The nonsymmetric Gaussian failed to fit the PSOD file, while in the case of BSOD the accuracy of the fit was similar to that obtained using the JANUS distribution (Tables IV and V). For the third protein, PFK, the skewed Gaussian gave better results than the JANUS function. Interestingly,

Table III. Fluorescence Decay Parameters for Three Mixtures of Five Noninteracting Fluorophores^a

Sample	JANUS				Two exponentials				Lorentzian								
	χ^2	C (ns)	$w_L/2$ (ns)	$w_R/2$ (ns)	χ^2	τ_1 (ns)	τ_2 (ns)	α_1 (%)	χ^2	C (ns)	w (ns)						
Fig. 8a ($\rho_j = 0.4$)	1.0	2.16	-0.07	-0.02	-0.04	1.0	1.75	2.75	0.72	1.0	1.99	0.17					
			+0.10	+0.02	+0.06								+0.08	+0.12	+0.04	+0.09	+0.08
			-0.05	-0.02	-0.05								-0.14	-0.25	-0.05	-0.12	-0.09
Fig. 8b ($\rho_j = 2.6$)	1.0	1.97	0.10	0.26	0.26	1.2	1.98	3.40	0.79	1.4	2.20	0.44					
			+0.16	+0.02	+0.06								+0.10	+0.20	+0.06	+0.08	+0.20
			-0.20	-0.02	-0.09								-0.06	-0.31	-0.05	-0.11	-0.16
Fig. 8c ($\rho_j = 5.8$)	1.0	1.82	0.08	0.46	0.46	1.5	2.06	4.68	0.84	5.5	2.29	0.86					
			+0.08	+0.03	+0.12								+0.06	+0.38	+0.07	+0.12	+0.22

^a χ^2 : reduced chi-square value. C , τ_1 , τ_2 : center of the distribution or discrete lifetime value. α_1 : preexponential factor of the first component ($\alpha_1 + \alpha_2 = 1$). w_L , w_R , w : width of lifetime distribution.

a better fit was also obtained for a simulated double-exponential decay (line 2 in Table V), where, again, the JANUS model failed to fit the data.

In conclusion, nonsymmetric distribution of lifetimes offer new possibilities in the analysis of dynamic fluorescence data. At the moment this approach is strictly empirical, since a physical model explaining the origin of these distributions is still missing. However, having the same degrees of freedom of the double-exponential decay, both the JANUS and the skewed Gaussian are statistically more appropriate than the symmetric Lorentzian, when a comparison between the discrete and the continuously distributed model is required. For these functions the independence between the right and the left tails allows us to fit the data without fixing a priori the shape of the distribution, which is instead one of

the limiting steps of the traditional fits. In particular, the analysis of the simulations reported in this paper revealed that the advantage of the JANUS and the skewed Gaussian distributions is particularly evident when a strong asymmetry is present in the lifetime set, required to fit the data. Finally, the results obtained with three selected proteins, although rather preliminary, suggest that the two nonsymmetric functions have a complementary character which might provide a valid alternative to discrete models.

ACKNOWLEDGMENTS

The authors wish to thank Dr. Enrico Gratton for discussion and comments on the manuscript and Dr. Desideri for the gift of purified PSOD.

Table IV. Fluorescence Decay Parameters of Bovine SOD, Bacterial SOD, and PFK^a

Sample	JANUS				Two exponentials				Lorentzian								
	χ^2	C (ns)	$w_L/2$ (ns)	$w_R/2$ (ns)	χ^2	τ_1 (ns)	τ_2 (ns)	α_1 (%)	χ^2	C (ns)	w (ns)						
BSOD	1.3	1.70	-0.10	-0.02	-0.05	2.1	1.29	3.17	0.72	2.4	1.99	0.80					
			+0.09	+0.02	+0.05								+0.09	+0.23	+0.04	+0.10	+0.06
			-0.08	-0.02	-0.05								-0.09	-0.19	-0.04	-0.10	-0.07
PSOD	1.0	1.34	0.54	0.50	0.50	7.3	0.81	2.60	0.75	1.0	1.31	1.03					
			+0.11	+0.03	+0.04								+0.08	+0.31	+0.05	+0.09	+0.10
			-0.35	-0.21	-0.19								-0.06	-0.23	-0.04	-0.41	-0.15
PFK	6.0	4.71	2.23	0.60	0.60	1.2	1.28	4.98	0.27	17	3.64	1.36					
			+0.50	+0.32	+0.12								+0.05	+0.18	+0.03	+0.22	+0.23

^a χ^2 : reduced chi-square value. C , τ_1 , τ_2 : center of the distribution or discrete lifetime value. α_1 : preexponential factor of the first component ($\alpha_1 + \alpha_2 = 1$). w_L , w_R , w : width of the lifetime distribution.

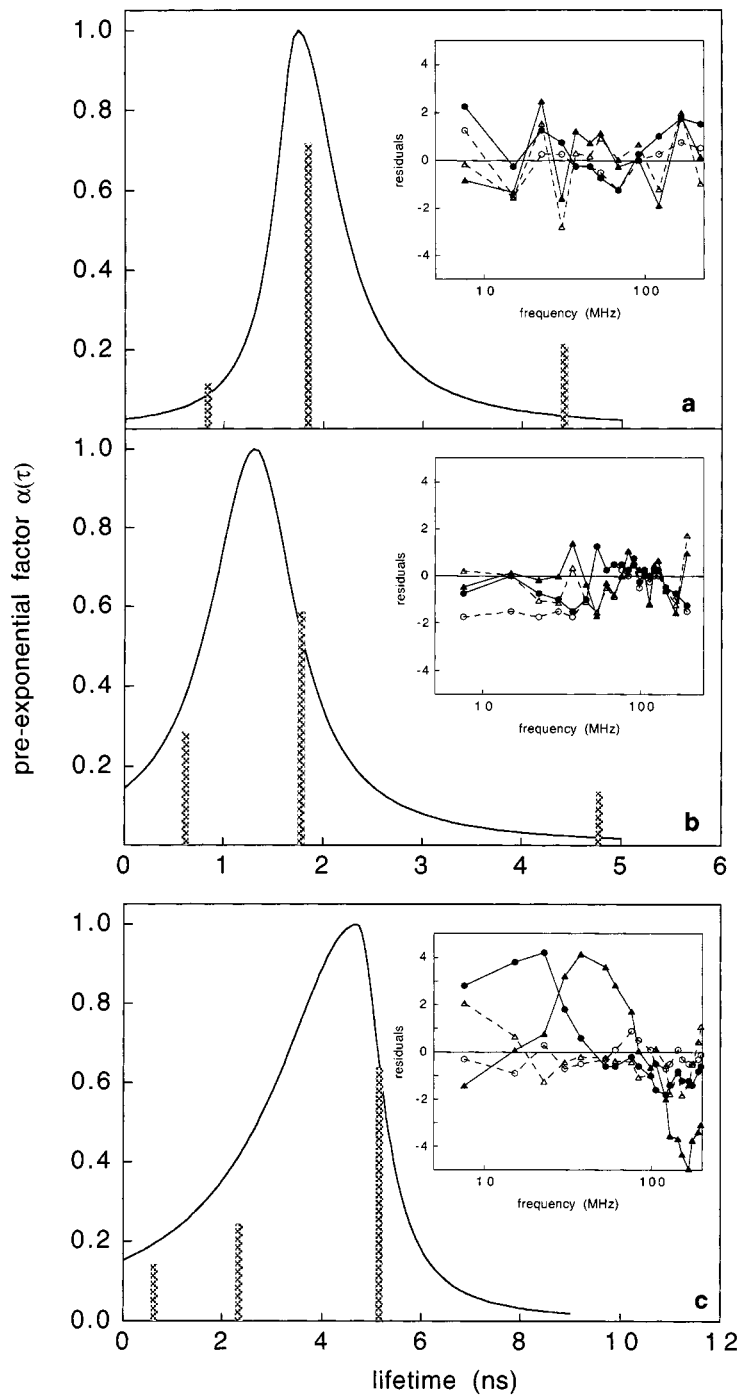


Fig. 9. Fluorescence lifetimes of BSOD (a), PSOD (b), and PFK (c), obtained with the JANUS function (solid line) and a three-exponential model (bars). Inset: The phase (triangles) and modulation (circles) residuals are reported as a function of the frequency modulation of the laser source in the case of the JANUS function (solid line, filled symbols) and a three-exponential model (dashed line, open symbols).

Table V. Fluorescence Decay Parameters for the Skewed Gaussian Function^a

Sample	χ^2	S	C (ns)	w (ns)
JANUS (Fig. 1b)	20	3.28 ± 0.45	0.81 ± 0.08	3.50 ± 0.11
Two exponentials (Fig. 2b)	1.5	2.19 ± 0.16	0.58 ± 0.02	1.54 ± 0.04
Lorentzian (Fig. 3b)	27	4.08 ± 0.08	0.46 ± 0.04	3.28 ± 0.08
Fig. 8a	1.1	1.42 ± 0.04	1.66 ± 0.05	0.88 ± 0.03
Fig. 8b	1.1	2.72 ± 0.04	1.56 ± 0.03	1.19 ± 0.03
Fig. 8c	3.2	3.42 ± 0.06	1.31 ± 0.04	1.81 ± 0.06
BSOD	1.7	3.36 ± 0.47	0.70 ± 0.05	1.74 ± 0.04
PSOD	5.2	2.43 ± 0.12	0.30 ± 0.05	1.27 ± 0.13
PFK	1.5	-0.62 ± 0.06	4.55 ± 0.41	3.52 ± 0.36

^a χ^2 : reduced chi-square value. S , C , w : skewness, center, and width of the distribution.

REFERENCES

1. J. R. Lakowicz and I. Gryczynski (1991) in J. R. Lakowicz (Ed.), *Topics in Fluorescence Spectroscopy*, Plenum Press, New York and London, Vol. 1, pp. 293–335.
2. S. Swaminathan, G. Krishnamoorthy, and N. Periasamy (1994) *Biophys. J.* **67**, 2013–2023.
3. A. Siemiarz, B. D. Wagner, and W. R. Ware (1990) *J. Phys. Chem.* **94**, 1661–1666.
4. J. M. Shaver and L. B. McGown (1996) *Anal. Chem.* **68**, 9–17.
5. J. R. Alcala, E. Gratton, and F. G. Prendergast (1987) *Biophys. J.* **51**, 587–596.
6. J. R. Alcala, E. Gratton, and F. G. Prendergast (1987) *Biophys. J.* **51**, 597–604.
7. J. R. Lakowicz, H. Cherek, I. Gryczynski, N. Joshi, and M. L. Johnson (1987) *Biophys. Chem.* **28**, 35–50.
8. W. Wiczak, P. S. Eis, M. N. Fishman, M. L. Johnson, and J. R. Lakowicz (1991) *J. Fluoresc.* **1**, 273–286.
9. E. Bismuto, E. Gratton, and G. Irace (1988) *Biochemistry* **27**, 2132–2136.
10. M. R. Eftink, I. Gryczynski, W. Wiczak, G. Laczko, and J. R. Lakowicz (1991) *Biochemistry* **30**, 8945–8953.
11. S. H. Grossman (1991) *Biophys. J.* **59**, 590–597.
12. G. Mei, N. Rosato, N. Silva, R. Rusch, E. Gratton, I. Savini, and A. Finazzi Agrò (1992) *Biochemistry* **31**, 7224–7230.
13. S. Ferreira, L. Stella, and G. Gratton (1994) *Biophys. J.* **66**, 1185–1196.
14. Z. Gryczynski, J. Lubkowski, and E. Bucci (1995) *J. Biol. Chem.* **270**, 19232–19237.
15. M. K. Helms, C. E. Petersen, N. V. Bhagavan, and D. M. Jameson (1997) *FEBS Lett.* **408**, 67–70.
16. E. Bismuto, G. Irace, S. D'Auria, M. Rossi, and R. Nucci (1997) *Eur. J. Biochem.* **244**, 53–58.
17. A. Di Venere, G. Mei, G. Gilardi, N. Rosato, F. De Matteis, R. McKay, E. Gratton, and A. Finazzi Agrò (1998) *Eur. J. Biochem.* **257**, 337–343.
18. F. Malvezzi Campeggi, M. E. Stroppolo, G. Mei, N. Rosato, and A. Desideri (1999) *Arch. Biochem. Biophys.* **370**, 201–207.
19. A. Di Venere, A. Rossi, F. De Matteis, N. Rosato, A. Finazzi Agrò, and G. Mei (2000) *J. Biol. Chem.* **275**, 3915–3921.
20. J. R. Alcala, E. Gratton, and F. G. Prendergast (1987) *Biophys. J.* **51**, 925–936.
21. E. Gratton and M. Limkeman (1983) *Biophys. J.* **44**, 315–324.
22. P. R. Bevington (1969) *Data Reduction and Error Analysis*, McGraw–Hill, New York.
23. M. Fisz (1963) *Probability Theory and Mathematical Statistics*, Wiley, New York and London, pp. 445–449.
24. S. J. Kim, F. N. Chowdhury, W. Stryjowski, E. S. Younathan, P. S. Russo, and M. D. Barkley (1993) *Biophys. J.* **65**, 215–226.
25. W. R. Ware (1992) in V. Ramamurthy (Ed.), *Photochemistry in Organized and Costrained Media*, VCA, New York, pp. 563–602.